




Article

Calculation of Stationary Magnetic Fields Based on the Improved Quadrature Formulas for a Simple Layer Potential

Igor Reznichenko ¹, Primož Podržaj ^{1,*} and Aljoša Peperko ^{1,2}¹ Faculty of Mechanical Engineering, University of Ljubljana, 1000 Ljubljana, Slovenia; ir4016@student.uni-lj.si (I.R.); aljosa.peperko@fs.uni-lj.si (A.P.)² Institute of Mathematics, Physics and Mechanics, 1000 Ljubljana, Slovenia

* Correspondence: primoz.podrzaj@fs.uni-lj.si

Abstract: This research deals with precision calculations of stationary magnetic fields of volumetric bodies. The electrostatics analogy allows for the use of a scalar magnetic potential, which reformulates the original task as a boundary value problem for the Laplace equation. We approach this with the boundary element method, specifically in distance ranges close to the magnetized surface, where existing standard numerical methods are known to struggle. This work presents an approach based on the improved quadrature formulas for the simple layer potential and its normal derivative. Numerical tests confirm significant improvements in calculating the field at any distance from the surface of the magnet.

Keywords: boundary element method; magnetic fields; numerical integration; Laplace equation; Fredholm integral equation

MSC: 35J05; 35J25; 35Q60; 45E05; 65D30; 65D32; 65M38



Citation: Reznichenko, I.; Podržaj, P.; Peperko, A. Calculation of Stationary Magnetic Fields Based on the Improved Quadrature Formulas for a Simple Layer Potential. *Mathematics* **2024**, *12*, 21. <https://doi.org/10.3390/math12010021>

Academic Editors: Zhuojia Fu, Yiqian He and Hui Zheng

Received: 9 November 2023

Revised: 12 December 2023

Accepted: 19 December 2023

Published: 21 December 2023



Copyright: © 2023 by the authors. Licensee MDPI, Basel, Switzerland. This article is an open access article distributed under the terms and conditions of the Creative Commons Attribution (CC BY) license (<https://creativecommons.org/licenses/by/4.0/>).

1. Introduction

In order to accurately simulate and control a magnetic system, one needs a reliable way of obtaining the values of the fields involved. This research deals with calculations of stationary magnetic fields at close proximity to a magnetized object. Standard numerical methods in the 3D case are known to struggle when the point of interest shifts towards the surface of the object. In order to achieve an adequate representation of the field under such conditions, one may need to heavily reduce the size of mesh elements, which greatly increases computational costs. The boundary element method approach is a valid choice, since it is known to yield a significant benefit because of the unit reduction in the dimensions of the original system of equations. Here, we aim to develop a calculation approach that provides uniform convergence and uniform approximation of stationary magnetic fields, that is, at any distance from the surface.

Magnetic fields are used in various physical applications [1]. Coil design is crucial in magnetic resonance imaging [2]. In transcranial magnetic stimulation, coils are used for individualized field targeting. A magnetically induced electric field is adopted to modulate brain tissue activity as a means of non-invasive scanning technology. Computational optimization of coil placement improves the performance of such medical imaging systems [3]. Linearized models are widely used to determine controller parameters of magnetic systems. However, the settings of a model usually fluctuate in relation to the operating point. A robust closed-loop control strategy for systems with active magnetic bearings requires calculations of the mentioned parameters over the entirety of the operating range [4]. Precision calculations of magnetic fields are required to successfully implement complicated magnetic phenomena, like magnetic levitation [5,6]. A more detailed expression of the magnetic force is an important optimization approach to controlling open-loop unstable

magnetic systems [5]. Overall, magnets are parts of various mechanical systems and are still studied with new methods [7,8].

All these devices go through a design stage where it is in the best interest of the developer to find out more about the future performance of magnetic components. This is the reason why various calculation techniques are used in magnetism, like the finite element method, variational computing, the boundary element method and so on. For simple surfaces and volumetric bodies, quite often, there exist explicit expressions for the magnetic fields of such objects. A symmetry axis, for example, reduces the dimensions of the problem and thus makes it much easier to acquire an exact formula. An infinite dimension of a body like the infinitely long cylinder often used in theoretical endeavors allows for a limit passage. Real magnetic objects, on the other hand, often possess complicated geometries. For this reason, numerical methods are the only means of calculation in such situations. But even in numerical calculations, one can see that standard quadrature formulas have their limitations and may diverge under certain conditions [9]. Therefore, the development of numerical methods that provide uniform approximation is important.

The Boundary Element Method

When modeling a physical process, the main efforts are usually aimed at solving differential equations that characterize a physical system in a specific area, whose boundaries may have a complex shape. The presence of complex boundaries in practice does not allow for the construction of an explicit solution to the problem, so numerical methods have become the only means of obtaining sufficient results. Standard numerical methods often consider differential equations directly in the form in which they are obtained, without special mathematical transformations [10]. In the finite difference method (FDR), differential operators are approximated by simpler algebraic (difference) operators acting in a sequence of nodes located in the region of interest. The finite element method (FEM) approximates the desired solution in the area under consideration by a sum of elements that are not infinitely small. However, there is a range of tasks in which these approaches face certain difficulties. Since accuracy directly depends on the density of the grid that determines the nodal points, a need to discretize an entire region of interest may lead to a large number of finite elements [11]. The resulting systems of a high order may be too large even for modern computers. This is especially noticeable in external three-dimensional problems, for example, in acoustic wave scattering [12].

The boundary element method (BEM) is viewed by many as a bit rarer alternative to the dominating approaches, like FEM and FDR. It is a collection of numerical methods for solving various boundary value problems for differential and integral equations [13]. A layer potential transforms the original problem into a boundary integral equation, which means that we only have to discretize the boundaries of the area of interest. Since a numerical solution to a boundary integral equation is usually found as a solution to a system of algebraic equations, the dimensions of the problem are reduced by one. When using the BEM for external boundary value problems, one does not need to stretch the calculation mesh for large distances, as it satisfies the conditions at infinity by default. This decrease in many applied problems has a decisive influence on the choice of this solution method [1,14,15]. Some researchers aim to combine, where possible, the benefits of both finite and boundary element methods [16,17].

The BEM is also known as the potential or the boundary integral equation method. It uses the principle of superposition. Simple and double layer potentials are used to prove the existence of solutions to boundary value problems for the Laplace and Helmholtz equations in simply connected domains [18,19]. It is a process of transition from the original problem to the integral Fredholm equation of the second kind [20]. The numerical algorithm for solving boundary value problems with layer potentials consists of two stages. First, we need to find the values of the potential density on the surface. These values are the numerical solutions to the boundary integral equation. Next, they are substituted into a

quadrature formula for the designated layer potential; thus, we find the solution to the boundary value problem at any point in space.

Standard quadrature formulas for the simple layer potential for the Laplace equation do not provide uniform approximation and convergence. When reaching the surface where the potential density is defined, the values of the simple layer potential tend to infinity, wherein the simple layer potential is a continuous function everywhere, including the surface itself. Thus, the property of boundedness and continuity of the potential on the surface [9] is not satisfied. The insufficient accuracy in calculating potentials near the surface using standard quadrature formulas is called the boundary layer effect [21]. The problem of calculating surface potentials near singularity points is widely known [22,23]. The article [24] discusses the need to move from standard numerical integration formulas to more advanced ones when calculating surface potentials near the surface on which the potential density is specified.

In [25], a quadrature formula for the simple layer potential which preserves the property of continuity was obtained. Unlike standard formulas of numerical integration, the developed method provides uniform convergence and uniform approximation when moving the point of interest through a given surface. This provides additional accuracy at close proximity without the need for mesh refinement. In [26], this approach was applied to obtain a quadrature formula for the direct value of the normal derivative of the simple layer potential. It can be applied to solving boundary integral equations that occur when dealing with various problems in mathematical physics. This research applies these results to the physical task of determining stationary magnetic fields in a three-dimensional case. We are going to see if these formulas should be used to numerically determine the magnetic potential at any point in 3D space.

2. Materials and Methods

2.1. Electrostatics Analogy: A Scalar Magnetic Potential

A permanent magnet can be viewed as a collection of the so-called imaginary magnetic charges. The idea behind it is the analogy between the electrostatic and magnetostatic fields [1]. If the area of interest does not possess conduction currents, $\sum \mathbf{j} = 0$, then $\operatorname{div} \mathbf{B} = 0$, and

$$\mathbf{B} = \mu_0(\mathbf{H} + \mathbf{M}), \quad (1)$$

where \mathbf{B} is the magnetic flux density vector, μ_0 is the vacuum permeability, \mathbf{H} is the magnetic field strength vector and \mathbf{M} is the magnetization vector. Then, the density of imaginary magnetic charges ρ_m can be formally introduced as

$$\operatorname{div} \mathbf{B} = \mu_0(\operatorname{div} \mathbf{H} - \rho_m) = 0. \quad (2)$$

Since $\operatorname{rot} \mathbf{H} = \mathbf{j}$ and $\mathbf{j} = 0$,

$$\begin{cases} \operatorname{div} \mathbf{H} = -\operatorname{div} \mathbf{M} = \rho_m, \\ \operatorname{rot} \mathbf{H} = 0. \end{cases} \quad (3)$$

Now, let us compare (3) with the electrostatic equations

$$\begin{cases} \operatorname{div} \mathbf{E} = \frac{\rho}{\epsilon_0}, \\ \operatorname{rot} \mathbf{E} = 0, \end{cases} \quad (4)$$

where ρ is the density of electrical charges and ϵ_0 is the dielectric permeability of vacuum. There is an analogy between Equations (3) and (4). The original magnetostatic problem can be addressed as an equivalent problem of electrostatics. The solution to (4) with constitutions $\mathbf{E} \rightarrow \mathbf{H}$ and $\rho/\epsilon_0 \rightarrow \rho_m$ is the solution to the original problem in (3).

If magnetization vector \mathbf{M} is constant, then $\rho_m = 0$. However, one also needs to consider the surface imaginary magnetic charge density (σ_m). It can be defined as

$$\sigma_m = (\mathbf{n}, \mathbf{M}_2 - \mathbf{M}_1), \quad (5)$$

where \mathbf{M}_1 and \mathbf{M}_2 are the magnetization vectors of media 1 and 2, with \mathbf{n} being the normal vector from the first to the second area (see Figure 1).

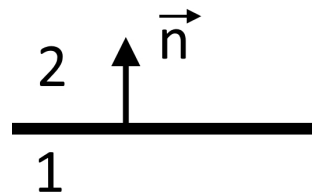


Figure 1. The normal vector (\mathbf{n}) between the two magnetized media (\mathbf{M}_1 and \mathbf{M}_2).

So, if surface magnetization is presented in this method, we also have to formally constitute $\sigma/\epsilon_0 \rightarrow \sigma_m$, where σ is the density of the surface electric charges. Also, if in the electrostatic solution we also estimate polarization vector \mathbf{P} , then $\mathbf{P}/\epsilon_0 \rightarrow \mathbf{M}$ is also required. The same formal procedure can be constructed for a magnetic field induced by stationary currents.

After solving the analogous electrostatic problem, the formal substitution is in place:

$$\begin{cases} \mathbf{E} \rightarrow \mathbf{H}, \\ \rho/\epsilon_0 \rightarrow \rho_m, \\ \sigma/\epsilon_0 \rightarrow \sigma_m, \\ \mathbf{P}/\epsilon_0 \rightarrow \mathbf{M} \end{cases} \quad (6)$$

which gives the solution to the original magnetostatic problem.

Let us assume the absence of free currents and that the electric fields (\mathbf{E}) (if any) present in the area of interest are constant. A scalar magnetic potential (u) is analogous to an electric potential. It is used to determine the field of a permanent magnet when its magnetization is known. Potential u uniquely provides the magnetic field at a given point in space. In a magnetic levitation train, for example, the field is determined in the vicinity of the accelerating channel [27]. A scalar magnetic potential (u) is introduced, so the magnetic field is found as

$$\mathbf{B} = -\text{grad } u. \quad (7)$$

This is appropriate when the free currents and the gradient of electric field \mathbf{E} are absent or can be neglected.

2.2. Exterior Neumann Boundary Value Problem for the Laplace Equation in a Three-Dimensional Domain

Let us introduce in space the Cartesian coordinate system $x = (x_1, x_2, x_3) \in \mathbb{R}^3$. We consider a simple, smooth, closed surface Γ of class C^2 enclosing a simply connected inner region D . Let the electric fields (if any) in region D be constant. The normal component of the magnetic flux vector (\mathbf{B}_n) is set as a boundary condition and is assumed to be a continuous function on Γ . Let us study an exterior Neumann boundary value problem for the Laplace equation.

$$\begin{cases} \Delta u = 0, & u \in C^1(\overline{\mathbb{R}^3 \setminus D}) \cap C^2(\mathbb{R}^3 \setminus \overline{D}), \\ \frac{\partial u(x)}{\partial \mathbf{n}} \Big|_{\Gamma} = f(x), & x \in \Gamma, f(x) \in C^1(\Gamma), \\ u = O\left(\frac{1}{|x|}\right), & |x| \rightarrow +\infty, \end{cases} \quad (8)$$

where $\partial/\partial \mathbf{n}$ is the normal derivative [20] on surface Γ from the outside at a point x . We assume that $u(x)$ has a normal derivative on Γ . The solution is found in the form of a simple layer potential $\mathcal{V}_0[\mu](x)$.

$$\mathcal{V}_0[\mu](x) = \frac{1}{4\pi} \int_{y \in \Gamma} \mu(y) \frac{1}{|x - y|} dS_y, \quad (9)$$

where $\mu = \mu(y) \in C^0(\Gamma)$ is the potential density. The simple layer potential $\mathcal{V}_0[\mu](x)$ is a harmonic function in the region $\mathbb{R}^3 \setminus \bar{D}$.

The normal derivative from the outside of surface Γ is given by the expression [20,26]

$$\frac{1}{2}\mu(x) + \frac{\partial \mathcal{V}_0[\mu](x)}{\partial \mathbf{n}_x} \Big|_{\Gamma}, \quad x \in \Gamma, \quad (10)$$

where

$$\frac{\partial \mathcal{V}_0[\mu](x)}{\partial \mathbf{n}_x} = \frac{1}{4\pi} \int_{\Gamma} \mu(y) \frac{\partial}{\partial \mathbf{n}_x} \frac{1}{|x-y|} dS_y \quad (11)$$

is the direct value of the normal derivative of the simple layer potential for the Laplace equation at a point $x \in \Gamma$, while \mathbf{n}_x is a unit normal directed inwardly. By equating this expression to the function defined on Γ , we obtain the following equation for the values of the potential density ($\mu(x)$):

$$\frac{1}{2}\mu(x) + \frac{\partial \mathcal{V}_0[\mu](x)}{\partial \mathbf{n}_x} \Big|_{\Gamma} = f(x), \quad x \in \Gamma. \quad (12)$$

Equation (12) is a linear Fredholm integral equation of the second kind, which, under given assumptions, is known to be uniquely solvable [20,28].

2.3. Surface Parametrization

Consider the following parametrization of surface Γ :

$$\begin{aligned} y &= (y_1, y_2, y_3) \in \Gamma, \quad y_1 = y_1(u, v), \quad y_2 = y_2(u, v), \quad y_3 = y_3(u, v); \\ u &\in [0, A], \quad v \in [0, B]; \\ y_j(u, v) &\in C^2([0, A] \times [0, B]), \quad j = 1, 2, 3. \end{aligned} \quad (13)$$

Let us introduce N points u_n with step h on the segment $[0, A]$ and M points v_m with step H on the segment $[0, B]$ and consider a partition of the rectangle $[0, A] \times [0, B]$ (see Figure 2):

$$\begin{aligned} A &= Nh, \quad B = MH, \quad u_n = (n + 1/2)h, \quad n = 0, \dots, N-1; \\ v_m &= (m + 1/2)H, \quad m = 0, \dots, M-1. \end{aligned} \quad (14)$$

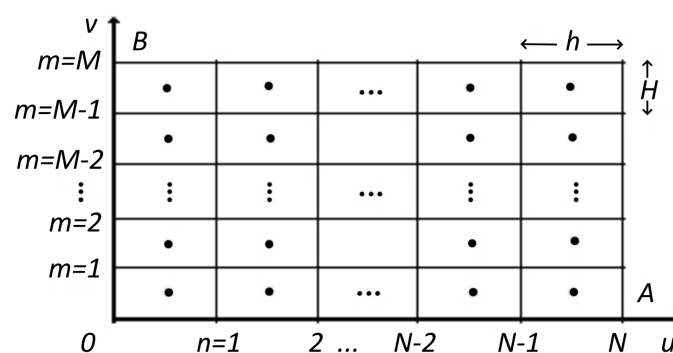


Figure 2. The rectangle $[0, A] \times [0, B]$ is divided into $N \times M$ small rectangles, whose centers are denoted as (u_n, v_m) and are used as reference points in Equation (12).

Let us introduce the continuous numbering of all of the small rectangles sized $h \times H$:

$$p = mN + n, \quad (15)$$

then, $0 \leq p \leq NM - 1$. If the number p is defined, then n, m are uniquely found as follows:

$$m = [p/N], \quad n = p - [p/N]N, \quad (16)$$

where $[\cdot]$ denotes the integer part of a non-negative real number. Under $y^p = y(u_n, v_m)$, $p = 0, 1, \dots, NM - 1$, we shall consider a central point of a small rectangle (u_n, v_m) , where n and m are determined by (16).

It is known that at a point $y = (y_1, y_2, y_3) \in \Gamma$, the components of a non-unit normal vector $\eta(y) = (\eta_1(y), \eta_2(y), \eta_3(y))$ can be expressed as matrix determinants by the expressions

$$\eta_1 = \begin{vmatrix} (y_2)_u & (y_3)_u \\ (y_2)_v & (y_3)_v \end{vmatrix}, \quad \eta_2 = \begin{vmatrix} (y_3)_u & (y_1)_u \\ (y_3)_v & (y_1)_v \end{vmatrix}, \quad \eta_3 = \begin{vmatrix} (y_1)_u & (y_2)_u \\ (y_1)_v & (y_2)_v \end{vmatrix}. \quad (17)$$

Let $|\eta(y)| = \sqrt{(\eta_1(y))^2 + (\eta_2(y))^2 + (\eta_3(y))^2}$. For a surface integral of the first kind, it is known that

$$\int_{\Gamma} F(y) ds_y = \int_0^A du \int_0^B F(y(u, v)) |\eta(y(u, v))| dv. \quad (18)$$

Note that if $|\eta(y(u, v))| = 0$ at some point, then the function $|\eta(y(u, v))|$ may be non-differentiable at this point. Therefore, we additionally require that

$$|\eta(y(u, v))| \in C^2([0, A] \times [0, B]). \quad (19)$$

In addition, we require that

$$|\eta(y(u, v))| > 0, \quad \forall (u, v) \in ((0, A) \times (0, B)). \quad (20)$$

With such parametrization of surface Γ , the simple layer potential with density $\mu(y) \in C^0(\Gamma)$ is expressed as

$$\begin{aligned} \mathcal{V}_0[\mu](x) &= \frac{1}{4\pi} \int_{\Gamma} \frac{\mu(y)}{|x - y|} ds_y = \frac{1}{4\pi} \int_0^A du \int_0^B \frac{\mu(y(u, v))}{|x - y(u, v)|} |\eta(y(u, v))| dv = \\ &= \frac{1}{4\pi} \sum_{n=0}^{N-1} \sum_{m=0}^{M-1} \int_{u_n-h/2}^{u_n+h/2} \int_{v_m-H/2}^{v_m+H/2} \frac{\mu(y(u, v))}{|x - y(u, v)|} |\eta(y(u, v))| dudv, \end{aligned} \quad (21)$$

where

$$|x - y(u, v)| = \sqrt{(x_1 - y_1(u, v))^2 + (x_2 - y_2(u, v))^2 + (x_3 - y_3(u, v))^2}.$$

On the other hand, the direct value of the normal derivative of the simple layer potential is expressed as

$$\begin{aligned} \frac{\partial \mathcal{V}_0[\mu](x)}{\partial \mathbf{n}_x} &= \frac{1}{4\pi} \int_{\Gamma} \mu(y) \frac{\partial}{\partial \mathbf{n}_x} \frac{1}{|x - y|} ds_y = -\frac{1}{4\pi |\eta(x)|} \times \\ &\times \int_0^A du \int_0^B \mu(y(u, v)) |\eta(y(u, v))| \sum_{j=1}^3 \frac{\eta_j(x)(x_j - y_j(u, v))}{|x - y(u, v)|^3} dv = \\ &= -\frac{1}{4\pi |\eta(x)|} \sum_{n=0}^{N-1} \sum_{m=0}^{M-1} \int_{u_n-h/2}^{u_n+h/2} du \int_{v_m-H/2}^{v_m+H/2} \mu(y(u, v)) |\eta(y(u, v))| \times \\ &\times \sum_{j=1}^3 \frac{\eta_j(x)(x_j - y_j(u, v))}{|x - y(u, v)|^3} dv. \end{aligned} \quad (22)$$

The double integrals in (21) and (22) are referred to as the canonical integrals. The numerical calculation of these expressions is the subject of rigorous research. In most applications, standard quadrature formulas of numerical integration are used for this task. But, as stated above, this approach struggles in ranges close to surface Γ . In this work, we are going to apply certain results in numerical methods [25,26] to the solution to the boundary value problem for the Laplace equation, which originates from the problem of finding the scalar magnetic potential. However, we shall use the standard formulas of numerical integration as a means of comparison.

2.4. Application of the Standard Quadrature Formulas for the Simple Layer Potential and Its Normal Derivative

The standard quadrature formula for the direct value of the simple layer potential on surface Γ is often used in applied calculations (Chapter 2, [9]) It is obtained by replacing the canonical integrals at points $x \neq y(u_{\hat{n}}, v_{\hat{m}})$ with their approximate values at the centers of the corresponding rectangles while zeroing the canonical integral over a piece of surface Γ centered at the point $x = y(u_{\hat{n}}, v_{\hat{m}})$

$$\left. \frac{\partial \mathcal{V}_0[\mu](x)}{\partial \mathbf{n}_x} \right|_{x=y(u_{\hat{n}}, v_{\hat{m}}) \in \Gamma} \approx \frac{1}{4\pi|\eta_{\hat{n}\hat{m}}|} \sum_{\substack{n=N-1, m=M-1 \\ n=0, m=0 \\ (n,m) \neq (\hat{n}, \hat{m})}} \mu_{nm} |\eta_{nm}| \mathcal{B}_{nm}(x), \quad (23)$$

where

$$\mathcal{B}_{nm}(x) = hH \sum_{j=1}^3 \frac{\eta_j(x)(y_j(u_n, v_m) - x_j)}{|x - y(u_n, v_m)|^3}. \quad (24)$$

Using continuous numbering (15), Formula (23) takes the form

$$\left. \frac{\partial \mathcal{V}_0[\mu](x)}{\partial \mathbf{n}_x} \right|_{x=y(u_{\hat{n}}, v_{\hat{m}}) \in \Gamma} \approx \frac{1}{4\pi|\eta_{\hat{p}}|} \sum_{\substack{p=0 \\ p \neq \hat{p}}}^{NM-1} \mu_p |\eta_p| \mathcal{B}_p(x), \quad (25)$$

where $\mu_p = \mu(y^p) = \mu_{nm}$ are the potential density values at the centers of small rectangles y^p and $\mathcal{B}_p(x) = \mathcal{B}_{nm}(x)$.

Thus, for a given parametrization of surface Γ , integral Equation (12) is reduced to a system of linear algebraic equations with respect to $N \cdot M$ values of the unknown potential density function $\mu(y^p) = \mu_p$ at points $y^p = y(u_n, v_m)$.

$$\frac{1}{2}\mu_{\hat{p}} + \frac{1}{4\pi|\eta_{\hat{p}}|} \sum_{\substack{p=0 \\ p \neq \hat{p}}}^{NM-1} \mu_p |\eta_p| \mathcal{B}_p^{\hat{p}} = f_{\hat{p}}, \quad \hat{p} = 0, 1, 2, \dots, NM-1, \quad (26)$$

where $f_{\hat{p}} = f(y^{\hat{p}})$ are the values of the boundary condition function on surface Γ and $\mathcal{B}_p(x) = \mathcal{B}_p(y(u_{\hat{n}}, v_{\hat{m}})) = \mathcal{B}_p(y^{\hat{p}}) = \mathcal{B}_p^{\hat{p}}$. Let us multiply system (26) by 4π and write it in the general form

$$\sum_{p=0}^{NM-1} \left(2\pi\Delta_p^{\hat{p}} + \frac{|\eta_p|}{|\eta_{\hat{p}}|} \mathcal{B}_p^{\hat{p}} (1 - \Delta_p^{\hat{p}}) \right) \mu_p = 4\pi f_{\hat{p}}, \quad (27)$$

where $\hat{p} = 0, 1, 2, \dots, NM-1$ and

$$\Delta_p^{\hat{p}} = \begin{cases} 1, & \text{if } p = \hat{p}, \\ 0, & \text{if } p \neq \hat{p}. \end{cases}$$

We multiply each \hat{p} -th equation of the system by $|\eta_{\hat{p}}|$

$$\sum_{p=0}^{NM-1} \left(2\pi|\eta_{\hat{p}}|\Delta_p^{\hat{p}} + |\eta_p|\mathcal{B}_p^{\hat{p}}(1 - \Delta_p^{\hat{p}}) \right) \mu_p = 4\pi|\eta_{\hat{p}}|f_{\hat{p}}, \quad (28)$$

where $\hat{p} = 0, 1, 2, \dots, NM-1$. Equation (28) can be written in matrix form as seen in (A1) in Appendix A. From this system of equations, we obtain the values of the potential density $\mu_{\hat{p}} = \mu(y^{\hat{p}})$ at the centers of small rectangles $y^{\hat{p}}$, which will then be used to calculate the simple layer potential everywhere outside Γ , thus solving the original boundary value problem.

To calculate the potential itself, as a means of comparison, we are going use the standard quadrature formula:

$$\mathcal{V}_0[\mu](x) \approx \frac{1}{4\pi} \sum_{n=0, m=0}^{n=N-1, m=M-1} \mu_{nm} \mathcal{D}_{nm}(x) = \frac{1}{4\pi} \sum_{p=0}^{NM-1} \mu_p \mathcal{D}_p(x), \quad (29)$$

where

$$\mathcal{D}_{nm} = \frac{hH|\eta(y(u_n, v_m))|}{|x - y(u_n, v_m)|}$$

and $\mathcal{D}_p(x) = \mathcal{D}_{nm}(x)$. It is obtained by replacing the canonical integrals at points $y(u_n, v_m) \in \Gamma$ to its approximate values at the centers of the corresponding rectangles. This formula, as we are going to see in the Results and Discussion section, tends to infinity when point x tends to the surface. In this case, the same is often true about more complex numerical integration formulas [9,24]. Thus, one of the ways to reduce the calculation error is the reduction in steps h, H which leads to a large number of boundary elements. This eliminates the main benefit of the boundary element method in close proximity to a surface [9].

2.5. Application of the Improved Quadrature Formulas for the Simple Layer Potential and Its Normal Derivative

In [26], a quadrature formula for the direct value of the normal derivative of the simple layer potential on surface Γ was explicitly obtained.

$$\begin{aligned} \frac{\partial \mathcal{V}_k[\mu](x)}{\partial \mathbf{n}_x} \Big|_{x=y(u_{\hat{n}}, v_{\hat{m}}) \in \Gamma} &\approx \frac{1}{4\pi} \mu_{\hat{n}\hat{m}} \mathcal{J}_{\hat{n}\hat{m}} + \frac{1}{4\pi|\eta(x)|} \times \\ &\times \sum_{\substack{n=N-1, m=M-1 \\ n=0, m=0 \\ (n,m) \neq (\hat{n}, \hat{m})}} \mu_{nm} |\eta(y(u_n, v_m))| T_{nm}(x), \end{aligned} \quad (30)$$

where the integrals $\mathcal{J}_{\hat{n}\hat{m}}$ and $T_{nm}(x)$ are calculated explicitly in [26]. Using continuous numbering (15), Formula (30) becomes

$$\begin{aligned} \frac{\partial \mathcal{V}_0[\mu](x)}{\partial \mathbf{n}_x} \Big|_{x=y(u_{\hat{n}}, v_{\hat{m}}) \in \Gamma} &\approx \frac{1}{4\pi} \mu_{\hat{n}\hat{m}} \mathcal{J}_{\hat{n}\hat{m}} + \frac{1}{4\pi|\eta_{\hat{n}\hat{m}}|} \sum_{\substack{n=N-1, m=M-1 \\ n=0, m=0 \\ (n,m) \neq (\hat{n}, \hat{m})}} \mu_{nm} |\eta_{nm}| T_{nm}(x) = \\ &= \frac{1}{4\pi} \mu_{\hat{p}} \mathcal{J}^{\hat{p}} + \frac{1}{4\pi|\eta_{\hat{p}}|} \sum_{\substack{p=0 \\ p \neq \hat{p}}}^{NM-1} \mu_p |\eta_p| T_p(x), \end{aligned} \quad (31)$$

where $\mu_p = \mu(y^p) = \mu_{nm}$ are the values of the potential density at the centers of small rectangles y^p , $T_p(x) = T_{nm}(x)$ and $|\eta_p| = |\eta(y^p)| = |\eta_{nm}|$ are the absolute values of the normal vector at y^p . The integral $\mathcal{J}^{\hat{p}} = \mathcal{J}_{\hat{n}\hat{m}}$, the density value $\mu_{\hat{p}} = \mu(y^{\hat{p}}) = \mu_{\hat{n}\hat{m}}$ and the absolute value of the normal vector $|\eta_{\hat{p}}| = |\eta(y^{\hat{p}})| = |\eta_{\hat{n}\hat{m}}|$ correspond to the case when point x lies in the region of integration. In this case, the integration is carried out over a small rectangle centered at the point $(u_{\hat{n}}, v_{\hat{m}})$, to which the dot $y^{\hat{p}} = y(u_{\hat{n}}, v_{\hat{m}}) = x$ on surface Γ corresponds.

Therefore, with the given parametrization of surface Γ , integral Equation (12) is reduced to the system of linear algebraic equations for $N \cdot M$ values of the unknown potential density function $\mu(y^p) = \mu_p$ at the points $y^p = y(u_n, v_m)$.

$$\frac{1}{2} \mu_{\hat{p}} + \frac{1}{4\pi} \mu_{\hat{p}} \mathcal{J}^{\hat{p}} + \frac{1}{4\pi|\eta_{\hat{p}}|} \sum_{\substack{p=0 \\ p \neq \hat{p}}}^{NM-1} \mu_p |\eta_p| T_p^{\hat{p}} = f_{\hat{p}}, \quad \hat{p} = 0, 1, 2, \dots, NM-1, \quad (32)$$

where $f_{\hat{p}} = f(y^{\hat{p}})$ are the values of the boundary condition function given on surface Γ , while $T_p(x) = T_p(y(u_{\hat{n}}, v_{\hat{m}})) = T_p(y^{\hat{p}}) = T_p^{\hat{p}}$. Here, we multiply system (32) by 4π and write it in a general form:

$$\sum_{p=0}^{NM-1} \left((\mathcal{J}^{\hat{p}} + 2\pi) \Delta_p^{\hat{p}} + \frac{|\eta_p|}{|\eta_{\hat{p}}|} T_p^{\hat{p}} (1 - \Delta_p^{\hat{p}}) \right) \mu_p = 4\pi f_{\hat{p}}, \quad (33)$$

where $\hat{p} = 0, 1, 2, \dots, NM-1$ and

$$\Delta_p^{\hat{p}} = \begin{cases} 1, & \text{if } p = \hat{p}, \\ 0, & \text{if } p \neq \hat{p}. \end{cases}$$

Next, each \hat{p} -th equation of system (33) is multiplied by $|\eta_{\hat{p}}|$.

$$\sum_{p=0}^{NM-1} \left(|\eta_{\hat{p}}| \left(\mathcal{J}^{\hat{p}} + 2\pi \right) \Delta_p^{\hat{p}} + |\eta_p| T_p^{\hat{p}} \left(1 - \Delta_p^{\hat{p}} \right) \right) \mu_p = 4\pi |\eta_{\hat{p}}| f_{\hat{p}}, \quad (34)$$

where $\hat{p} = 0, 1, 2, \dots, NM - 1$. Equation (34) can be written in matrix form as seen in (A2) in Appendix A. By reversing the matrix on the left side of the equality in (A2) and multiplying the inverse matrix on the left by the column with the values of the boundary condition function, we obtain the density value capacity $\mu_{\hat{p}} = \mu(y^{\hat{p}})$ at the centers of small rectangles $y^{\hat{p}}$, which will then be used to calculate the simple layer potential everywhere outside Γ , thereby solving the original boundary value problem.

To calculate the simple layer potential, we use the quadrature formula obtained in [25]

$$\mathcal{V}_0[\mu](x) \approx \frac{1}{4\pi} \sum_{n=0}^{N-1} \sum_{m=0}^{M-1} \mu_{nm} \theta_{nm}(x), \quad (35)$$

where the integral $\theta_{nm}(x)$ is explicitly derived in [25]. This formula preserves the property of continuity of the simple layer potential and approximates this function uniformly.

3. Results and Discussion

In [25], a quadrature formula for the simple layer potential which provides uniform approximation was obtained. A quadrature formula for the normal derivative of the simple layer potential with improved accuracy over standard numerical integration was suggested in [26]. We adopt these results to solve a particular magnetostatics problem, which is an external Neumann boundary value problem for the values of a scalar magnetic potential.

3.1. Numerical Tests

Testing was carried out for the case where surface Γ is a sphere of unit radius which is given parametrically by

$$y_1(u, v) = \cos u \sin v, \quad y_2(u, v) = \sin u \sin v, \quad y_3(u, v) = \cos v, \quad (36)$$

where $(u, v) \in [0, 2\pi] \times [0, \pi]$.

Test 1. Under a boundary condition of the form $f(x) = 3/5 \cdot P_2(\cos \vartheta)$, $x \in \Gamma$, the solution to the external Neumann boundary value problem for the Laplace equation is known and is given by the expression

$$u(x) = \frac{P_2(\cos \vartheta)}{5|x|^2} \text{ when } |x| > 1. \quad (37)$$

In this case, the density of the simple layer potential is equal to

$$\mu(x) = P_2(\cos \vartheta), \quad x \in \Gamma, \quad (38)$$

where ϑ is the zenith angle in spherical coordinates centered at the origin and

$$P_2(\cos \vartheta) = \frac{3 \cos^2 \vartheta - 1}{2}$$

is a Legendre polynomial.

Test 2. Under a boundary condition of the form $f(x) = 4/7 \cdot P_3(\cos \vartheta)$, $x \in \Gamma$, the solution to the external Neumann boundary value problem for the Laplace equation is known and is given by the expression

$$u(x) = \frac{P_3(\cos \vartheta)}{7|x|^3} \text{ when } |x| > 1. \quad (39)$$

In this case, the density of the simple layer potential is equal to

$$\mu(x) = P_3(\cos \vartheta), \quad x \in \Gamma, \quad (40)$$

where ϑ is the zenith angle in spherical coordinates centered at the origin and

$$P_3(\cos \vartheta) = \frac{5 \cos^3 \vartheta - 3 \cos \vartheta}{2}$$

is a Legendre polynomial.

Test 3. Under a boundary condition of the form $f(x) = 5/9 \cdot P_4(\cos \vartheta)$, $x \in \Gamma$, the solution to the external Neumann boundary value problem for the Laplace equation is known and is given by the expression

$$u(x) = \frac{P_4(\cos \vartheta)}{9|x|^4} \text{ when } |x| > 1. \quad (41)$$

In this case, the density of the simple layer potential is equal to

$$\mu(x) = P_4(\cos \vartheta), \quad x \in \Gamma, \quad (42)$$

where ϑ is the zenith angle in spherical coordinates centered at the origin and

$$P_4(\cos \vartheta) = \frac{35 \cos^4 \vartheta - 30 \cos^2 \vartheta + 3}{8}$$

is a Legendre polynomial.

Test 4. Under a boundary condition of the form $f(x) = 3/5 \cdot \cos 2\varphi \sin^2 \vartheta$, $x \in \Gamma$, the solution to the external Neumann boundary value problem for the Laplace equation is known and is given by the expression

$$u(x) = \frac{\cos 2\varphi \sin^2 \vartheta}{5|x|^2} \text{ when } |x| > 1. \quad (43)$$

In this case, the density of the simple layer potential is equal to

$$\mu(x) = \cos 2\varphi \sin^2 \vartheta, \quad x \in \Gamma, \quad (44)$$

where ϑ and φ are the zenith and azimuth angles in spherical coordinates centered at the origin.

Test 5. Under a boundary condition of the form $f(x) = 4/7 \cdot \cos 3\varphi \sin^3 \vartheta$, $x \in \Gamma$, the solution to the external Neumann boundary value problem for the Laplace equation is known and is given by the expression

$$u(x) = \frac{\cos 3\varphi \sin^3 \vartheta}{7|x|^3} \text{ when } |x| > 1. \quad (45)$$

In this case, the density of the simple layer potential is equal to

$$\mu(x) = \cos 3\varphi \sin^3 \vartheta, \quad x \in \Gamma, \quad (46)$$

where ϑ and φ are the zenith and azimuth angles in spherical coordinates centered at the origin.

Test 6. Under a boundary condition of the form $f(x) = 5/9 \cdot \cos 4\varphi \sin^4 \vartheta$, $x \in \Gamma$, the solution to the external Neumann boundary value problem for the Laplace equation is known and is given by the expression

$$u(x) = \frac{\cos 4\varphi \sin^4 \vartheta}{9|x|^4} \text{ when } |x| > 1. \quad (47)$$

In this case, the density of the simple layer potential is equal to

$$\mu(x) = \cos 4\varphi \sin^4 \vartheta, \quad x \in \Gamma, \quad (48)$$

where ϑ and φ are the zenith and azimuth angles in spherical coordinates centered at the origin.

3.2. Calculations of the Potential Density

The solution to the external Neumann boundary value problem by the described method consists of two stages. In the first stage, using one of the two given quadrature formulas for the direct value of the normal derivative of the simple layer potential, we obtain the values of the potential density μ_p , $p = 0, 1, \dots, NM - 1$, at the centers of small rectangles, solving the corresponding system of linear algebraic equations. This can be either quadrature Formula (31), constructed in [26], or the standard quadrature formula for the normal derivative of the simple layer potential in (25). The point coordinates that were used to estimate the maximum absolute error are (see Figure 3)

$$\begin{aligned} x_j^{q_l} &= y_j(u_q, v_l), \quad j = 1, 2, 3, \\ u_q &= \frac{2\pi}{2N}q, \quad q = 0, \dots, 2N; \quad v_l = \frac{\pi}{2M}l, \quad l = 1, \dots, 2M - 1, \end{aligned} \quad (49)$$

where $y_j(u, v)$ is determined by the expressions in (36). That is, these points are located on the unit sphere at the centers of the small rectangles (see Figure 2), the midpoints of the boundaries between them and the intersections of these boundaries. Note that these points are distributed over the entire unit sphere.

The calculations were carried out for various values of M and N . The step values are determined as $h = 2\pi/N$, $H = \pi/M$. If $N/2 = M = 10$, then $h = H \approx 0.31$; if $N/2 = M = 20$, then $h = H \approx 0.16$; if $N/2 = M = 40$, then $h = H \approx 0.079$.

First, let us consider the calculation error of potential density. The first number in the cells of Table 1 is the maximum absolute value of error of potential density μ_p , acquired with the standard quadrature Formula (25) for the normal derivative of the simple layer potential. The second number after the semicolon is the maximum absolute value of error of potential density μ_p , acquired with the improved quadrature Formula (31) for the normal derivative [26].

Table 1. The maximum absolute error of potential density in tests 1–3.

Test Number	$N/2 = M = 10$	$N/2 = M = 20$	$N/2 = M = 40$
Test 1	0.039; 0.015	0.021; 0.0096	0.019; 0.0057
Test 2	0.038; 0.014	0.02; 0.0091	0.018; 0.0055
Test 3	0.031; 0.014	0.019; 0.0088	0.018; 0.0054
Test 4	0.081; 0.0035	0.042; 0.0011	0.021; 0.0003
Test 5	0.087; 0.0038	0.044; 0.0014	0.022; 0.00039
Test 6	0.088; 0.0037	0.043; 0.0015	0.022; 0.00047

Let us also consider the average absolute error over all reference points (15) in Equation (12). The first number in the cells of Table 2 is the mean absolute error of potential density μ_p , acquired with the standard quadrature Formula (25). The second number (after the semicolon) is the mean absolute error of potential density μ_p , acquired with the improved quadrature Formula (31).

Table 2. The mean absolute error of potential density in tests 1–3.

Test Number	$N/2 = M = 10$	$N/2 = M = 20$	$N/2 = M = 40$
Test 1	0.023; 0.0043	0.013; 0.0014	0.0066; 0.00047
Test 2	0.02; 0.0041	0.012; 0.0013	0.0059; 0.00045
Test 3	0.018; 0.0045	0.01; 0.0014	0.0053; 0.00046
Test 4	0.024; 0.0012	0.012; 0.00035	0.0059; 9.5×10^{-5}
Test 5	0.023; 0.0011	0.011; 0.00036	0.0054; 9.9×10^{-5}
Test 6	0.021; 0.001	0.0099; 0.00036	0.0051; 0.00011

3.3. Calculations of the Potential—The Solution to the Neumann Problem

In the second stage, the obtained values of potential density μ_p are used to calculate the simple layer potential at any point in the region $\mathbb{R}^3 \setminus \overline{D}$ using one of the two formulas. It can be either (35) from [25] or the standard quadrature formula for the simple layer potential (29).

In the numerical tests, the values of potential density μ_p , obtained using the improved Formula (31), are only used in Formula (35). Similarly, the values of the potential density μ_p obtained using the standard Formula (25) we will use only in Formula (29).

The calculations of the simple layer potential solutions of the original external Neumann boundary value problem were carried out at some points on the auxiliary spheres with centers at the origin and radii $R = 1 + \Delta R$. Thus, the auxiliary spheres are outside of the sphere of unit radius, on which the boundary condition or the potential density is given, at a distance ΔR from it. Then, the values of absolute errors at these points were calculated. For each auxiliary sphere the maximum values of these errors are determined.

The point coordinates that were used to estimate the maximum absolute error are (see Figure 3)

$$\begin{aligned} x_j^{ql} &= Ry_j(u_q, v_l), \quad j = 1, 2, 3, \\ u_q &= \frac{2\pi}{2N}q, \quad q = 0, \dots, 2N; \quad v_l = \frac{\pi}{2M}l, \quad l = 1, \dots, 2M-1, \end{aligned} \quad (50)$$

where $y_j(u, v)$ is determined by the expressions in (36) and R is the auxiliary sphere radius.

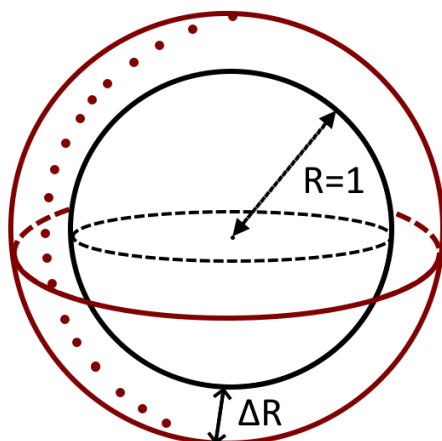


Figure 3. Points x on the test spheres of radii equal to $1 + \Delta R$ are chosen according to (50). The maximum values of absolute error of the simple layer potential among all of these points are used in Tables 3–8. If $\Delta R = 0$, then it is the first stage of the numerical solution, which is the determination of the potential density values (μ_p).

That is, these points are located at a distance ΔR outside of the unit sphere above the centers of the small rectangles (see Figure 2), the midpoints of the boundaries between them and the intersections of these boundaries. Note that these points are distributed over the entire sphere.

Table 3. Maximum absolute values of error of quadrature formulas in test 1.

ΔR	$N/2 = M = 10$	$N/2 = M = 20$	$N/2 = M = 40$
0.1	0.018; 0.013	0.0047; 0.0056	0.0021; 0.0018
0.06	0.039; 0.015	0.0077; 0.0077	0.0024; 0.0029
0.03	0.098; 0.016	0.02; 0.0094	0.004; 0.0045
0.01	0.35; 0.016	0.083; 0.01	0.017; 0.0056
0.001	3.86; 0.016	0.98; 0.01	0.24; 0.0058
0.0001	38.9; 0.016	9.97; 0.01	2.48; 0.0058

Table 4. Maximum absolute values of error of quadrature formulas in test 2.

ΔR	$N/2 = M = 10$	$N/2 = M = 20$	$N/2 = M = 40$
0.1	0.017; 0.011	0.0040; 0.0050	0.0010; 0.0016
0.06	0.030; 0.013	0.0069; 0.0070	0.0017; 0.0027
0.03	0.082; 0.014	0.015; 0.0087	0.0034; 0.0042
0.01	0.30; 0.014	0.066; 0.0094	0.013; 0.0054
0.001	3.36; 0.014	0.80; 0.0094	0.19; 0.0056
0.0001	33.9; 0.014	8.18; 0.0094	2.01; 0.0056

Table 5. Maximum absolute values of error of quadrature formulas in test 3.

ΔR	$N/2 = M = 10$	$N/2 = M = 20$	$N/2 = M = 40$
0.1	0.017; 0.011	0.0036; 0.0047	0.00076; 0.0015
0.06	0.028; 0.013	0.0065; 0.0067	0.0014; 0.0026
0.03	0.059; 0.014	0.014; 0.0083	0.0031; 0.0041
0.01	0.22; 0.014	0.058; 0.0090	0.012; 0.0053
0.001	2.4; 0.014	0.70; 0.0090	0.18; 0.0055
0.0001	24.2; 0.014	7.19; 0.0090	1.84; 0.0055

Table 6. Maximum absolute values of error of quadrature formulas in test 4.

ΔR	$N/2 = M = 10$	$N/2 = M = 20$	$N/2 = M = 40$
0.1	0.020; 0.015	0.0098; 0.015	0.012; 0.015
0.06	0.065; 0.010	0.0067; 0.010	0.0069; 0.010
0.03	0.19; 0.0068	0.033; 0.0057	0.0035; 0.0055
0.01	0.70; 0.010	0.16; 0.0026	0.032; 0.0021
0.001	7.74; 0.015	1.96; 0.0035	0.48; 0.00044
0.0001	78.2; 0.016	20; 0.0041	4.96; 0.00097

Table 7. Maximum absolute values of error of quadrature formulas in test 5.

ΔR	$N/2 = M = 10$	$N/2 = M = 20$	$N/2 = M = 40$
0.1	0.022; 0.012	0.0065; 0.01	0.0077; 0.0099
0.06	0.067; 0.0095	0.0055; 0.0073	0.0046; 0.0069
0.03	0.19; 0.0072	0.033; 0.0045	0.0028; 0.0039
0.01	0.72; 0.013	0.16; 0.0024	0.031; 0.0016
0.001	7.97; 0.018	1.98; 0.0041	0.48; 0.00049
0.0001	80.5; 0.019	20.1; 0.0047	4.97; 0.0011

Table 8. Maximum absolute values of error of quadrature formulas in test 6.

ΔR	$N/2 = M = 10$	$N/2 = M = 20$	$N/2 = M = 40$
0.1	0.020; 0.019	0.012; 0.015	0.013; 0.015
0.06	0.062; 0.016	0.010; 0.011	0.0086; 0.010
0.03	0.19; 0.013	0.028; 0.0069	0.0055; 0.0061
0.01	0.72; 0.017	0.15; 0.0034	0.030; 0.0024
0.001	7.98; 0.022	1.88; 0.0049	0.47; 0.00067
0.0001	80.6; 0.022	19.2; 0.0055	4.92; 0.0013

The calculations were carried out for various values of M and N . The step values were determined as $h = 2\pi/N$, $H = \pi/M$. If $N/2 = M = 10$, then $h = H \approx 0.31$; if $N/2 = M = 20$, then $h = H \approx 0.16$; if $N/2 = M = 40$, then $h = H \approx 0.079$.

Now, let us consider the calculation error of the solution to the external Neumann boundary problem. The first numbers in the cells of Tables 3–8 are the maximum absolute values of error of the solution, acquired with the standard quadrature formula for the simple layer potential (29). The second numbers after the semicolon are the maximum absolute

values of error of the solution, acquired with the improved quadrature Formula (35) for the simple layer potential [25].

Table 1 shows that the maximum absolute values of error of potential density μ_p , acquired with the improved quadrature Formula (31) from [26], are a few times lower than those of the standard quadrature Formula (25). The same can be observed about the mean absolute values of error of potential density in Table 2, while in tests 4–6, the values acquired with the improved quadrature Formula (31) are lower by an order of magnitude. In both tables, Formula (31) shows the first order of convergence in H for tests 1–3 and the third order of convergence in H for tests 4–6.

Let us perform an estimate of the maximum absolute value of error of the numerical solution to the original problem in tests 1–6 from Tables 3–8. From them, it follows that the standard Formula (29) for the simple layer potential does not provide uniform approximation and uniform convergence of the solution in the form of the simple layer potential, since at a fixed step H , the error tends to infinity when approaching surface Γ . That is why this formula is not the priority choice for solving boundary value problems for the Laplace equation near a surface Γ .

Quadrature Formula (35) provides uniform approximation of the solution to the original problem. This remains true even for increasingly oscillating test functions, like in test 3 or 6. Therefore, Formula (35) retains the property of continuity of the simple layer potential while heading towards surface Γ . This is why both Formulas (31) and (35) should be used for numerically solving various boundary value problems for the Laplace equation, like the scalar magnetic potential.

4. Conclusions

1. In this work, a new method for determining three-dimensional stationary magnetic fields is proposed. Based on the conception of a magnetic potential, this task can be formulated as a boundary value problem for the Laplace equation with a Neumann condition on a magnetized surface. This work presents a full solution using the boundary element method (BEM). With the use of a simple layer potential, a three-dimensional magnetostatic problem is reduced to a two-dimensional boundary Fredholm integral equation that is uniquely solvable.
2. While, in an external boundary value problem, the BEM automatically satisfies the conditions at infinity, it is known to struggle in close proximity to the boundary. The non-integrable singularity is addressed by applying the improved quadrature formulas for the simple layer potential (35) and its normal derivative (31) [25,26]. For the values of the potential density, a system of linear algebraic equations was constructed, the matrix form of which can be seen in Appendix A. For the same task, standard quadrature Formulas of numerical integration were used as a reference.
3. With the mean and maximum absolute values of error of the potential density being significantly lower (up to an order of magnitude) than that, when acquired with the standard approach, Formula (31) shows improved accuracy. The improved Formula (35) for the simple layer potential provides uniform approximation of the solution, unlike the standard Formula (29), which tends to infinity. The developed approach provides improved accuracy and approximates to the solution uniformly at any distance from the surface, as was confirmed with numerical tests. This remains true even for increasingly oscillating test functions. Therefore, the developed approach can be used to solve the magnetostatic problem at any distance from a volumetric body.

Author Contributions: Conceptualization, I.R., P.P. and A.P.; methodology, I.R., P.P. and A.P.; software, I.R.; validation, I.R., P.P. and A.P.; formal analysis, I.R.; investigation, I.R.; resources, I.R., P.P. and A.P.; data curation, I.R., P.P. and A.P.; writing—original draft preparation, I.R.; writing—review and editing, I.R., P.P. and A.P.; visualization, I.R., P.P. and A.P.; supervision, P.P. and A.P. All authors have read and agreed to the published version of the manuscript.

Funding: P. Podržaj was supported by Slovenian Research Agency, grant number P2-0270. A. Peperko was partially supported by ARIS-Slovenian Agency for Research and Innovation (grants P1-0222 and J2-2512).

Data Availability Statement: The data used in this research are available from the corresponding author upon reasonable request.

Conflicts of Interest: The authors declare no conflict of interest.

Appendix A

Here, we write system (28) in matrix form:

$$\begin{pmatrix} 2\pi|\eta_0| & |\eta_1|\mathcal{B}_1^0 & \cdots & |\eta_{\hat{p}-1}|\mathcal{B}_{\hat{p}-1}^0 & |\eta_{\hat{p}}|\mathcal{B}_{\hat{p}}^0 & |\eta_{\hat{p}+1}|\mathcal{B}_{\hat{p}+1}^0 & \cdots & |\eta_{NM-1}|\mathcal{B}_{NM-1}^0 \\ |\eta_0|\mathcal{B}_0^1 & 2\pi|\eta_1| & \cdots & |\eta_{\hat{p}-1}|\mathcal{B}_{\hat{p}-1}^1 & |\eta_{\hat{p}}|\mathcal{B}_{\hat{p}}^1 & |\eta_{\hat{p}+1}|\mathcal{B}_{\hat{p}+1}^1 & \cdots & |\eta_{NM-1}|\mathcal{B}_{NM-1}^1 \\ \vdots & \vdots & \ddots & \vdots & \vdots & \vdots & \vdots & \vdots \\ \vdots & \vdots & \vdots & \ddots & \vdots & \vdots & \vdots & \vdots \\ |\eta_0|\mathcal{B}_0^{\hat{p}} & |\eta_1|\mathcal{B}_1^{\hat{p}} & \cdots & |\eta_{\hat{p}-1}|\mathcal{B}_{\hat{p}-1}^{\hat{p}} & 2\pi|\eta_{\hat{p}}| & |\eta_{\hat{p}+1}|\mathcal{B}_{\hat{p}+1}^{\hat{p}} & \cdots & |\eta_{NM-1}|\mathcal{B}_{NM-1}^{\hat{p}} \\ |\eta_0|\mathcal{B}_0^{\hat{p}+1} & |\eta_1|\mathcal{B}_1^{\hat{p}+1} & \cdots & |\eta_{\hat{p}-1}|\mathcal{B}_{\hat{p}-1}^{\hat{p}+1} & |\eta_{\hat{p}}|\mathcal{B}_{\hat{p}}^{\hat{p}+1} & 2\pi|\eta_{\hat{p}+1}| & \cdots & |\eta_{NM-1}|\mathcal{B}_{NM-1}^{\hat{p}+1} \\ \vdots & \vdots & \vdots & \vdots & \vdots & \vdots & \ddots & \vdots \\ |\eta_0|\mathcal{B}_0^{NM-1} & |\eta_1|\mathcal{B}_1^{NM-1} & \cdots & |\eta_{\hat{p}-1}|\mathcal{B}_{\hat{p}-1}^{NM-1} & |\eta_{\hat{p}}|\mathcal{B}_{\hat{p}}^{NM-1} & |\eta_{\hat{p}+1}|\mathcal{B}_{\hat{p}+1}^{NM-1} & \cdots & 2\pi|\eta_{NM-1}| \end{pmatrix} \times$$

$$\times \begin{pmatrix} \mu_0 \\ \mu_1 \\ \vdots \\ \mu_{NM-1} \end{pmatrix} = 4\pi \begin{pmatrix} |\eta_0|f_0 \\ |\eta_1|f_1 \\ \vdots \\ |\eta_{NM-1}|f_{NM-1} \end{pmatrix}. \quad (\text{A1})$$

Also, let us write system (34) in matrix form:

$$\begin{pmatrix} |\eta_0|(\mathcal{J}^0 + 2\pi) & |\eta_1|T_1^0 & \cdots & |\eta_{\hat{p}-1}|T_{\hat{p}-1}^0 & |\eta_{\hat{p}}|T_{\hat{p}}^0 & |\eta_{\hat{p}+1}|T_{\hat{p}+1}^0 & \cdots & |\eta_{NM-1}|T_{NM-1}^0 \\ |\eta_0|T_0^1 & |\eta_1|(\mathcal{J}^1 + 2\pi) & \cdots & |\eta_{\hat{p}-1}|T_{\hat{p}-1}^1 & |\eta_{\hat{p}}|T_{\hat{p}}^1 & |\eta_{\hat{p}+1}|T_{\hat{p}+1}^1 & \cdots & |\eta_{NM-1}|T_{NM-1}^1 \\ \vdots & \vdots & \ddots & \vdots & \vdots & \vdots & \vdots & \vdots \\ \vdots & \vdots & \vdots & \ddots & \vdots & \vdots & \vdots & \vdots \\ |\eta_0|T_0^{\hat{p}} & |\eta_1|T_1^{\hat{p}} & \cdots & |\eta_{\hat{p}-1}|T_{\hat{p}-1}^{\hat{p}} & |\eta_{\hat{p}}|(\mathcal{J}^{\hat{p}} + 2\pi) & |\eta_{\hat{p}+1}|T_{\hat{p}+1}^{\hat{p}} & \cdots & |\eta_{NM-1}|T_{NM-1}^{\hat{p}} \\ |\eta_0|T_0^{\hat{p}+1} & |\eta_1|T_1^{\hat{p}+1} & \cdots & |\eta_{\hat{p}-1}|T_{\hat{p}-1}^{\hat{p}+1} & |\eta_{\hat{p}}|T_{\hat{p}}^{\hat{p}+1} & |\eta_{\hat{p}+1}|(\mathcal{J}^{\hat{p}+1} + 2\pi) & \cdots & |\eta_{NM-1}|T_{NM-1}^{\hat{p}+1} \\ \vdots & \vdots & \vdots & \vdots & \vdots & \vdots & \ddots & \vdots \\ |\eta_0|T_0^{NM-1} & |\eta_1|T_1^{NM-1} & \cdots & |\eta_{\hat{p}-1}|T_{\hat{p}-1}^{NM-1} & |\eta_{\hat{p}}|T_{\hat{p}}^{NM-1} & |\eta_{\hat{p}+1}|T_{\hat{p}+1}^{NM-1} & \cdots & |\eta_{NM-1}|(\mathcal{J}^{NM-1} + 2\pi) \end{pmatrix} \times$$

$$\times \begin{pmatrix} \mu_0 \\ \mu_1 \\ \vdots \\ \mu_{NM-1} \end{pmatrix} = 4\pi \begin{pmatrix} |\eta_0|f_0 \\ |\eta_1|f_1 \\ \vdots \\ |\eta_{NM-1}|f_{NM-1} \end{pmatrix}. \quad (\text{A2})$$

References

1. Reznichenko, I.; Podržaj, P.; Peperko, A. Control theory and numerical analysis of magnetic field involving mechanical systems. In Proceedings of the 17th International Symposium on Operational Research in Slovenia, SOR'23, Slovenian Society Informatika (SSI), Section for Operational Research (SOR), Bled, Slovenia, 20–22 September 2023.
2. Cobos Sanchez, C.; Power, H.; Garcia, S.G.; Rubio Bretones, A. Quasi-static multi-domain inverse boundary element method for MRI coil design with minimum induced E-field. *Eng. Anal. Bound. Elem.* **2011**, *35*, 264–272. [\[CrossRef\]](#)
3. Gomez, L.J.; Dannhauer, M.; Peterchev, A.V. Fast computational optimization of TMS coil placement for individualized electric field targeting. *NeuroImage* **2021**, *228*, 117696. [\[CrossRef\]](#) [\[PubMed\]](#)

4. Polajžer, B.; Štumberger, G.; Ritonja, J.; Dolinar, D. Variations of Active Magnetic Bearings Linearized Model Parameters Analyzed by Finite Element Computation. *IEEE Trans. Magn.* **2008**, *44*, 1534–1537. [\[CrossRef\]](#)
5. Reznichenko, I.; Podržaj, P. Design Methodology for a Magnetic Levitation System Based on a New Multi-Objective Optimization Algorithm. *Sensors* **2023**, *23*, 979. [\[CrossRef\]](#) [\[PubMed\]](#)
6. Chen, Q.; Li, J. Field Dynamic Balancing for Magnetically Suspended Turbomolecular Pump. *Sensors* **2023**, *23*, 6168. [\[CrossRef\]](#) [\[PubMed\]](#)
7. Pashkovskiy, A.; Tkachev, A.; Bahvalov, U. New Standard Elements for Calculating Magnetic Fields of Electromechanical and Magnetic Systems with Permanent Magnets. In Proceedings of the 2018 International Conference on Industrial Engineering, Applications and Manufacturing (ICIEAM), Moscow, Russia, 15–18 May 2018; pp. 1–5. [\[CrossRef\]](#)
8. Yu, Y.; Yue, H.; Wen, F.; Zhao, H.; Zhou, A. Electromagnetic Force on an Aluminum Honeycomb Sandwich Panel Moving in a Magnetic Field. *Sensors* **2023**, *23*, 8577. [\[CrossRef\]](#) [\[PubMed\]](#)
9. Brebbia, C.A.; Telles, J.C.F.; Wrobel, L.C. *Boundary Element Techniques Theory and Applications in Engineering*; Springer: Berlin/Heidelberg, Germany, 1984.
10. Samarskii, A.A.; Nikolaev, E.S. *Numerical Methods for Grid Equations*; Birkhauser: Basel, Switzerland, 1989.
11. Samarskii, A.A.; Matus, P.P.; Vabishchevich, P.N. *Difference Schemes with Operator Factors*; Springer: Berlin/Heidelberg, Germany, 2010.
12. Colton, D.; Kress, R. *Integral Equation Methods in Scattering Theory*; John Wiley & Sons: New York, NY, USA, 1983.
13. Banerjee, P.; Butterfield, R. *Boundary Element Methods in Engineering Science*; McGraw-Hill Inc.: London, UK, 1981.
14. Kalitkin, N.N.; Alshina, E.A. *Numerical Methods: Numerical Analysis*; Academia: Moscow, Russia, 2013.
15. Kalitkin, N.N.; Koryakin, P.V. *Numerical Methods: Mathematical Physics*; Academia: Moscow, Russia, 2013.
16. Lobry, J. A FEM-Green Approach for Magnetic Field Problems with Open Boundaries. *Mathematics* **2021**, *9*, 1662. [\[CrossRef\]](#)
17. Radcliffe, A. Quasi-Stable, Non-Magnetic, Toroidal Fluid Droplets in a Ferrofluid with Annular Magnetic Field. *Magnetism* **2022**, *2*, 380–391. [\[CrossRef\]](#)
18. Sun, Y.; Wei, X.; Zhuang, Z.; Luan, T. A Numerical Method for Filtering the Noise in the Heat Conduction Problem. *Mathematics* **2019**, *7*, 502. [\[CrossRef\]](#)
19. Sun, Y.; Hao, S. A Numerical Study for the Dirichlet Problem of the Helmholtz Equation. *Mathematics* **2021**, *9*, 1953. [\[CrossRef\]](#)
20. Vladimirov, V.S. *Equations of Mathematical Physics*; Mir Publishers: Moscow, Russia, 1981.
21. Khatri, S.; Kim, A.; Cortez, R.; Carvalho, C. Close evaluation of layer potentials in three dimensions. *J. Comput. Phys.* **2020**, *423*, 109798. [\[CrossRef\]](#)
22. Klockner, A.; Barnett, A.; Greengard, L.; O’Neil, M. Quadrature by expansion: A new method for the evaluation of layer potentials. *J. Comput. Phys.* **2013**, *252*, 332–349. [\[CrossRef\]](#)
23. Epstein, C.L.; Greengard, L.; Klockner, A. On the convergence of local expansions of layer potentials. *Siam J. Numer. Anal.* **2013**, *51*, 2660–2679. [\[CrossRef\]](#)
24. Af Klinteberg, L.; Sorgentone, C.; Tornberg, A.K. Quadrature error estimates for layer potentials evaluated near curved surfaces in three dimensions. *Comput. Math. Appl.* **2022**, *111*, 1–19. [\[CrossRef\]](#)
25. Krutitskii, P.A.; Fedotova, A.D.; Kolybasova, V.V. Quadrature formula for the simple layer potential. *Differ. Equations* **2019**, *55*, 1226–1241. [\[CrossRef\]](#)
26. Krutitskii, P.A.; Reznichenko, I.O.; Kolybasova, V.V. Quadrature formula for the direct value of the normal derivative of the single layer potential. *Differ. Equations* **2020**, *56*, 1237–1255. [\[CrossRef\]](#)
27. Han, H.S.; Kim, D.S. *Magnetic Levitation: Maglev Technology and Applications*; Springer: Berlin/Heidelberg, Germany, 2016.
28. Krutitskii, P.A. A mixed problem for the Laplace equation in three-dimensional multiply connected domains. *Differ. Equ.* **1999**, *35*, 1193–1200.

Disclaimer/Publisher’s Note: The statements, opinions and data contained in all publications are solely those of the individual author(s) and contributor(s) and not of MDPI and/or the editor(s). MDPI and/or the editor(s) disclaim responsibility for any injury to people or property resulting from any ideas, methods, instructions or products referred to in the content.